ICA 2016 BUENOS AIRES
Buenos Aires – 5 to 9 September 2016
Acoustics for the 21st Century...

PROCEEDINGS of the 22nd International Congress on Acoustics

Aircraft Noise - Aeroacoustics: Paper ICA2016-93

Flow-induced noise regimes of a wall-mounted finite airfoil

Danielle J. Moreau[(a)], **Con J. Doolan**[(b)]

[(a)]School of Mechanical and Manufacturing Engineering, UNSW Australia, d.moreau@unsw.edu.au
[(b)]School of Mechanical and Manufacturing Engineering, UNSW Australia, c.doolan@unsw.edu.au

Abstract

Flow interaction with a wall-mounted finite airfoil is a major noise source in a number of practical aerodynamic and hydrodynamic situations including turbomachinery blade and end-wall flows, aircraft wing and body junction flows and ship appendage and hull junction flows. In all of these cases, the flow around the wall-mounted finite airfoil is three-dimensional with boundary layer impingement at the airfoil-wall junction and flow over the tip. An experimental investigation has been conducted in an anechoic wind tunnel to define the noise characteristics of a wall-mounted finite airfoil with a flat ended tip in cross-flow. This paper describes the wall-mounted finite airfoil noise generation mechanisms and how flow over an airfoil can create tonal or broadband noise. Examples of vortex shedding as well as tonal and broadband noise spectra are presented along with aeroacoustic beamforming sound maps which provide information about the airfoil noise generation mechanisms and noise source locations in each regime.

Keywords: Airfoil noise; trailing edge noise; beamforming.

Flow-induced noise regimes of a wall-mounted finite airfoil

1 Introduction

Unsteady fluid flow and airfoils are common partners in industry that often create unwanted sound. Examples include submarine hydrofoils mounted to a hull, wind turbine blades mounted to a hub or the stators in an aeroengine that are connected to an outer wall. These technologies all employ an airfoil that is wall-mounted and finite in length with boundary layer impingement at the airfoil-wall junction and flow over the tip. While noise production of a two-dimensional or semi-infinite airfoil is well documented [1–4], only limited attention has been paid to the flow-induced noise of a wall-mounted finite airfoil [5, 6].

The aim of this paper is to provide an overview of the noise produced by a wall-mounted finite airfoil. Some current research results of an experimental program to study wall-mounted finite airfoil noise in the Stability Wind Tunnel at Virginia Tech are presented. The experimental dataset given in this paper includes trailing edge noise spectra and sound maps taken with a microphone array for a wall-mounted finite airfoil with rectangular planform. The aspect ratio of the airfoil is $L/C = 3$ where the L is span and C is chord. Measurements are presented at a range of chord based Reynolds numbers ($Re_C = 7.9 \times 10^5 - 1.6 \times 10^6$) and two angles of attack ($\alpha = 0^\circ$ and 6°).

2 Experimental Methodology

Experiments were performed in the anechoic test section of the Stability Wind Tunnel at Virginia Tech [7]. This facility has low turbulence levels of up to 0.03% and can achieve flow speeds of up to 80 m/s depending on blockage. The test section has dimensions of 1.83 m $\times$ 1.83 m $\times$ 7.3 m and is shown in Fig. 1 (a). The test section has tensioned Kevlar walls that contain the flow while being acoustically transparent. Sound generated in the test section passes through the Kevlar walls into two anechoic chambers located on either side of the test section where acoustic instrumentation can be placed.

The test model consisted of a finite length NACA 0012 airfoil with flat ended tip. The airfoil has a chord of $C = 0.4$ m, a span of $L = 1.2$ m and an aspect ratio of $L/C = 3$. As shown in Fig. 1 (b), the airfoil was flush mounted to the wind tunnel ceiling so that the airfoil length axis (span) was perpendicular to the direction of the flow. Tests were performed with the airfoil (1) untripped so that natural boundary transition may occur and (2) tripped on both sides using serrated trip tape with 0.5 mm thickness at 10% chord.

Experiments were conducted at free-stream velocities of $U_\infty = 30 - 60$ m/s corresponding to Reynolds numbers based on airfoil chord of $Re_C = 7.9 \times 10^5 - 1.6 \times 10^6$. Measurements were taken for an airfoil angle of attack of $\alpha = 0^\circ$ and 6°. An AVEC microphone array located in the port anechoic chamber was used to measure the sound emitted by the wall-mounted finite airfoil. The array has an outer diameter of 1.1 m and its centre was positioned 0.93 m above the

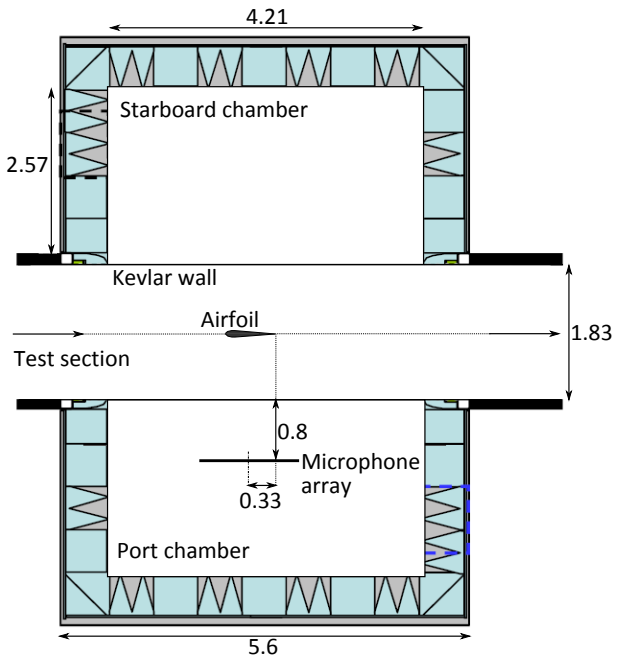

(a) Top view of the anechoic test section [7].

(b) Test model.

Figure 1: **Experimental setup in the Stability Wind Tunnel. Dimensions in m.**

test section floor. The location of the microphone array relative to the airfoil is shown in Fig. 1 (a). The array consists of 117 Panasonic model WM-64PNT Electret microphones arranged in a 9-armed spiral. The 117 microphones were connected to an AVEC designed signal conditioning and filtering box and two 64-channel PCI-based data acquisition cards. Data from the 117 microphones were acquired at a sampling frequency of 51,200 Hz for a sample time of 32 s. Maps of local sound pressure contributions (or sound maps) were obtained using AVEC's post-processing algorithm and are displayed in 1/12th octave bands. In addition to sound maps, 1/12th octave band trailing edge noise spectra have been estimated by integrating the sound map over the trailing edge region. This integration process yields the sound pressure level as measured at the microphone array centre due to the sources contained in the integration region. The sound map trailing edge integration region is shown in Fig. 2. In this figure, x is the streamwise direction where the flow is from left to right and y is the spanwise direction. A position of $x = 0$, $y = 0$ corresponds to the centre of the test section.

To characterize the incoming flow conditions, Table 1 states the boundary layer thickness of the incoming boundary layer at flow speeds of $U_\infty = 30 - 60$ m/s, estimated skin friction coefficient, c_f, and the ratios of side plate boundary layer thickness to airfoil thickness and length [6]. Table 1 shows that in this study, the incoming boundary layer thickness is between 5.67% and 6.08% of the airfoil length.

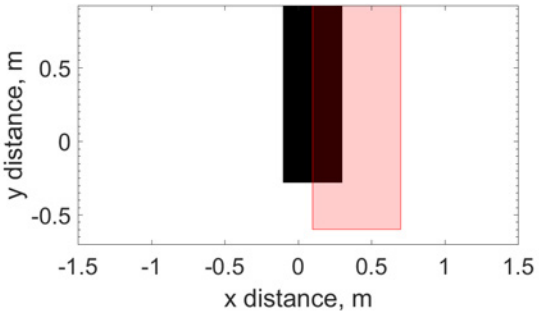

Figure 2: **Sound map 1/12th octave band trailing edge integration region (shown in red) for the wall-mounted airfoil (shown in black). The flow is from left to right.**

Table 1: **Incoming wall boundary layer properties.**

U_∞, m/s	Re_C	δ, mm	Re_δ	c_f	δ/T	δ/L
30	7.9×10^5	73	1.5×10^5	0.00257	1.52	0.0608
40	1.1×10^6	71	1.9×10^5	0.00252	1.48	0.0592
50	1.3×10^6	70	2.3×10^5	0.00246	1.46	0.0583
60	1.6×10^6	68	2.7×10^5	0.00243	1.42	0.0567

3 Results

Figures 3 and 4 present integrated trailing edge spectra and sound maps for the wall-mounted finite airfoil. The sound maps in Fig. 4 are presented at the top flow speed of $U_\infty = 60$ m/s only. Sound maps are given in 1/12th octave band center frequencies of 1-4.5 kHz and the location of the airfoil is shown in white.

The sound maps in Fig. 4 show the dominant noise source location is the airfoil trailing edge at all frequencies above 1 kHz when the airfoil boundary layer is in both a turbulent and natural state. Despite the boundary layer height being only being 6% of the airfoil span, junction noise is the dominant noise mechanism at a frequency of 1 kHz. The junction noise source is located at the airfoil leading edge in Fig. 4 (a), (b) and (c), suggesting that the interaction of boundary layer vorticity with the leading edge is responsible for low-frequency noise.

Turbulent boundary layer trailing edge noise spectra for the wall-mounted finite airfoil are given in Fig. 3 (a) and (b). These spectra are broadband in nature and follow a clear trend with noise levels decreasing with a reduction in flow velocity. In the mid-frequency range (e.g. at 2 kHz at $U_\infty = 60$ m/s), the airfoil trailing edge spectra display a broad peak. This peak reduces in frequency and amplitude with decreasing flow speed and is attributed to vortex shedding from the trailing edge.

According to Blake [3], blunt trailing edge vortex shedding noise is negligible if the trailing edge is sufficiently sharp such that the bluntness parameter $h/\delta^* < 0.3$ where h is the thickness of the trailing edge and δ^* is the boundary layer displacement thickness. In this study, the

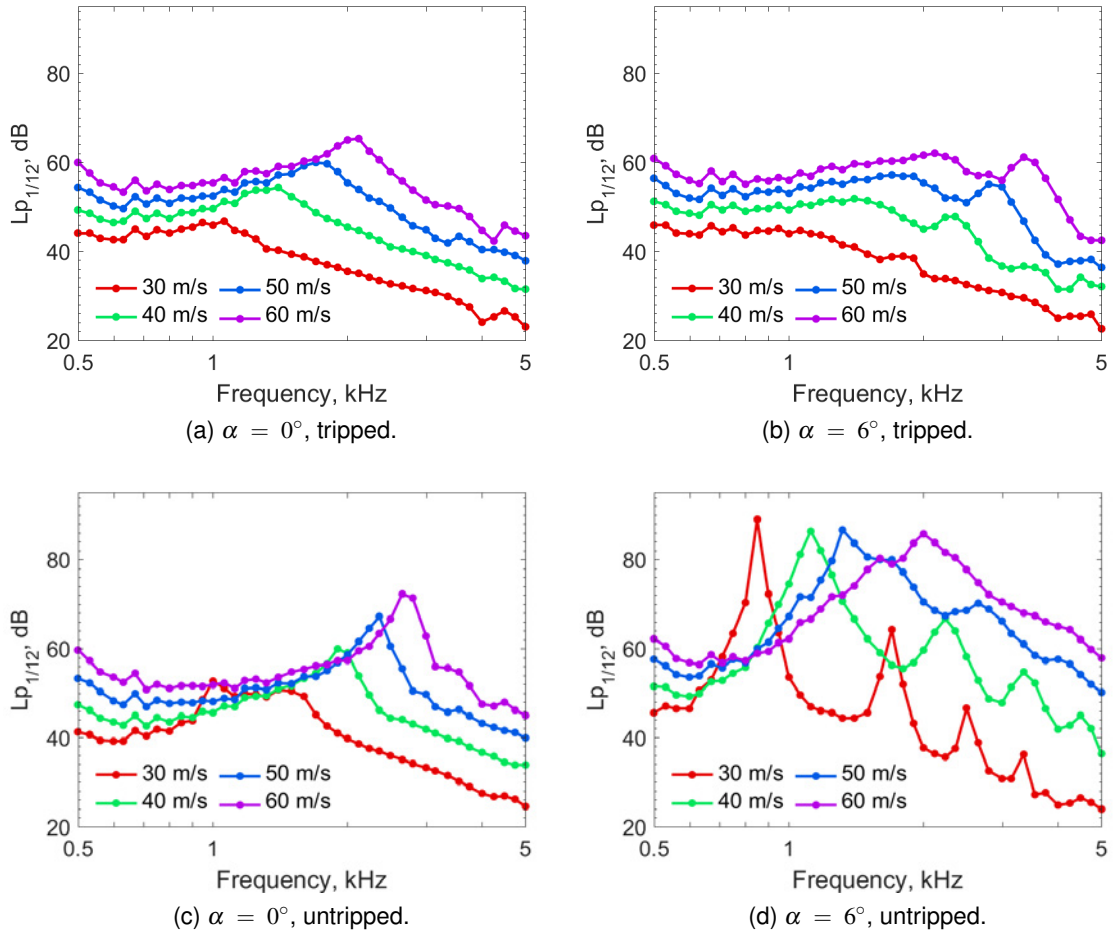

(a) $\alpha = 0°$, tripped. (b) $\alpha = 6°$, tripped.

(c) $\alpha = 0°$, untripped. (d) $\alpha = 6°$, untripped.

Figure 3: **1/12th octave band trailing edge noise spectra for the wall-mounted airfoil.**

boundary layer displacement thickness has been calculated using the panel method coupled integral boundary layer method code XFOIL [8]. The method employed here is to first calculate the spanwise effective angle of attack distribution for the wall-mounted finite airfoil using the general formulation of Prandtl's classical lifting-line theory for a rectangular planform wing [9]. The growth of the boundary layer over the surface of the wall-mounted finite airfoil was then modeled using XFOIL. The boundary layer displacement thickness was calculated at 2% intervals in the spanwise direction using the spanwise effective angle of attack distribution. As the trailing edge boundary layer displacement thickness varies over the airfoil span, the value used in this study is the average value over the span. The bluntness parameter h/δ^* was found to be well above 0.3 for all free-stream velocities and angles of attack in this study indicating that noise contributions due to blunt trailing edge vortex shedding can be expected. The sound maps in Fig. 4 (e) and (f) show that the airfoil trailing edge noise source is distributed along the entire airfoil span at the frequency of blunt vortex shedding noise contributions (e.g. at 2 kHz at $U_\infty = 60$ m/s) consistent with the proposed noise generation mechanism.

At frequencies of 2.65 kHz and above, the dominant noise source of the wall-mounted finite airfoil with tripped turbulent boundary layers is the trailing edge tip (see Fig. 4 (i), (j), (m), (n), (q) and (r)). The tip noise source is attributed to the formation of the tip vortex structure at the airfoil trailing edge-tip corner. The tip noise source is much stronger at the higher angle of attack of $\alpha = 6^\circ$ and manifests itself as a broad peak in the trailing edge noise spectra (e.g. at 3.7 kHz at $U_\infty = 60$ m/s in Fig. 3 (b)). The tip noise peak visible at $\alpha = 6^\circ$ reduces in frequency and amplitude with decreasing flow speed.

The trailing edge noise spectra for the wall-mounted finite airfoil with natural boundary layer transition are given in Fig. 3 (c) and (d). At $\alpha = 0^\circ$ the spectra display a low amplitude peak (e.g. at 2.65 Hz at $U_\infty = 60$ m/s in Fig. 3 (c)). Increasing the angle of attack to $\alpha = 6^\circ$ results in a number of high amplitude peaks in the noise spectra with level maxima that increase with decreasing velocity. The sound maps in Fig. 4 (g), (h), (k) and (l) show the trailing edge noise source responsible for these peak contributions is located at the airfoil's midspan.

The formation of the peaks in the trailing edge noise spectra of Fig. 3 (c) and (d) is attributed to instabilities known as Tollmien-Schlichting (T-S) waves that are present in a transitional boundary layer. Sound is produced by the scattering of these boundary layer instabilities at the trailing edge. The frequency distribution of T-S waves in the boundary layer is sensitive to small changes in Reynolds number and for this reason, flow speed variation is observed in the spectral shape and amplitude of the radiated noise. High amplitude tonal noise may also be produced if the boundary layer instabilities couple with acoustic feedback [2]. The large spectral peaks observed at $\alpha = 6^\circ$ in Fig. 3 (d) each contain a number of these narrowband tonal contributions.

As observed for the case of tripped turbulent boundary layers, the trailing edge tip is the dominant noise source location for the wall-mounted finite airfoil with natural boundary layer transition at high frequencies of 3.75 kHz and above (see Fig. 4 (o), (p), (s) and (t)). At 4.5 kHz, an additional noise source is also observed along the airfoil trailing edge in the junction and mid span region at $\alpha = 0^\circ$ and 6°, respectively (see Fig. 4 (s) and (t)).

For an idealized (non-compact) semi-infinite flat plate, the amplitude of the radiated trailing edge noise scales proportionally with M^5, where M is the free-stream Mach number [10]. Figure 5 shows the 1/12th octave band turbulent boundary layer trailing edge noise spectra for the wall-mounted finite airfoil normalised by

$$Lp_{1/12\ \text{scaled1}} = Lp_{1/12} - 50\log_{10}(M), \tag{1}$$

where $Lp_{1/12}$ is the far-field acoustic spectrum. The frequency of trailing edge noise is expected to scale according to $f \sim U_\infty/l$, where l is the characteristic length scale. In Fig. 5 (a) and (b), trailing edge thickness, h, is used as the characteristic length scale and the normalised spectra are plotted against Strouhal number based on trailing edge thickness, $St_h = fh/U_\infty$.

At $\alpha = 0^\circ$, Fig. 5 (a) shows that an M^5 power law gives a good collapse of the airfoil trailing edge noise spectra between $U_\infty = 30$ and 60 m/s. Spectral data that are originally spread by almost 30 dB are collapsed to within 8 dB. The level maxima of the noise spectra in Fig. 5 (a) all occur at a Strouhal number of $St_h = 0.106$. This is in good agreement with several other studies that have found blunt vortex shedding noise to occur at $St_h \approx 0.1$ [1, 4, 11].

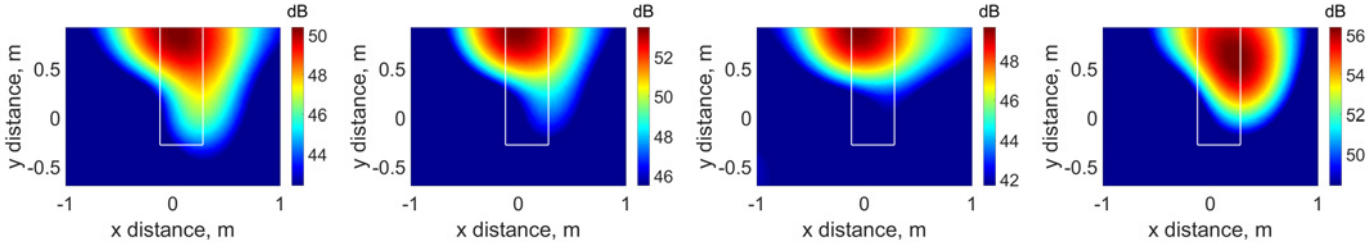

(a) 1 kHz, $0°$, tripped. (b) 1 kHz, $6°$, tripped. (c) 1 kHz, $0°$, untripped. (d) 1 kHz, $6°$, untripped.

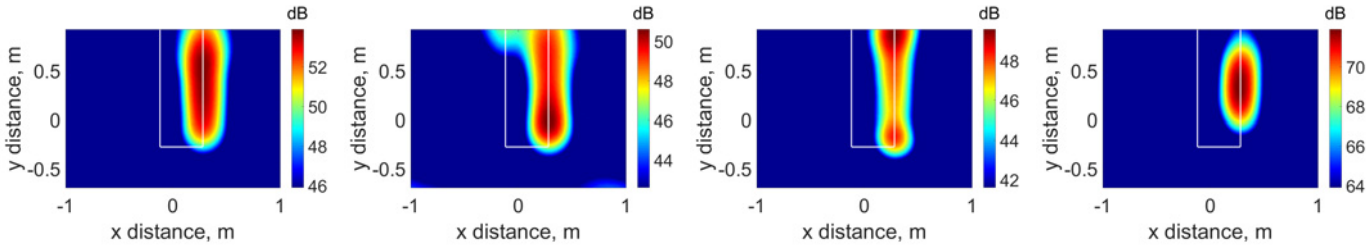

(e) 2 kHz, $0°$, tripped. (f) 2 kHz, $6°$, tripped. (g) 2 kHz, $0°$, untripped. (h) 2 kHz, $6°$, untripped.

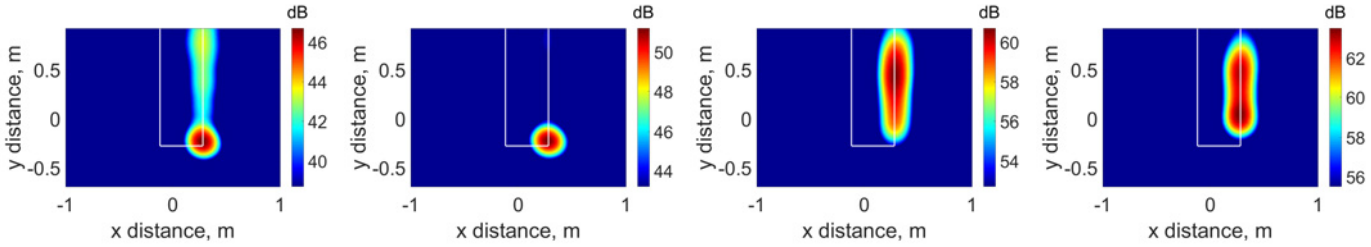

(i) 2.65 kHz, $0°$, tripped. (j) 2.65 kHz, $6°$, tripped. (k) 2.65 kHz, $0°$, untripped. (l) 2.65 kHz, $6°$, untripped.

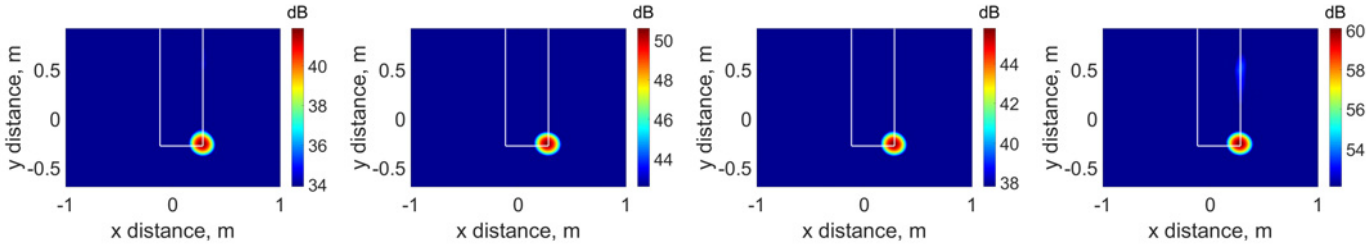

(m) 3.75 kHz, $0°$, tripped. (n) 3.75 kHz, $6°$, tripped. (o) 3.75 kHz, $0°$, untripped. (p) 3.75 kHz, $6°$, untripped.

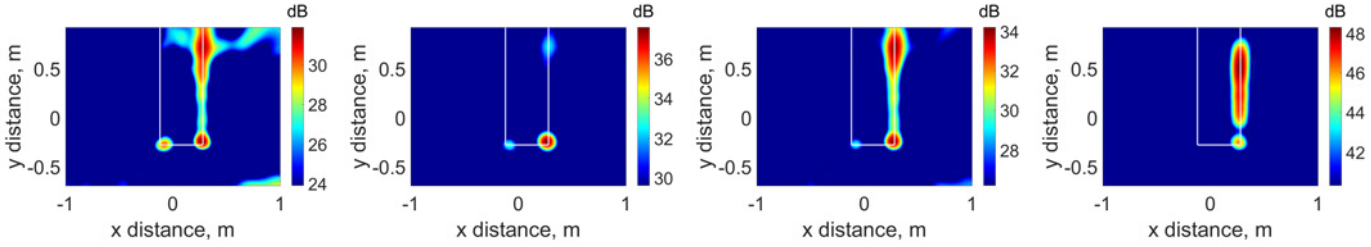

(q) 4.5 kHz, $0°$, tripped. (r) 4.5 kHz, $6°$, tripped. (s) 4.5 kHz, $0°$, untripped. (t) 4.5 kHz, $6°$, untripped.

Figure 4: **Sound maps for the wall-mounted finite airfoil at $U_\infty = 60$ m/s.**

Figure 5 (b) shows the spectra measured at $\alpha = 6°$ coalesce to within 8 dB with M^5 scaling. The peak noise level occurs at $St_h = 0.106$ and tip vortex formation noise peaks at $St_h = 0.168$. Tip vortex formation noise is observed to scale poorly with M^5 suggesting that the well known edge scattering scaling for trailing edge noise is not applicable to this noise generation mechanism.

A common parameter employed in trailing edge noise normalisation is boundary layer displacement thickness, δ^* [1]. As suggested by Brooks et al. [4], the 1/12th octave band turbulent boundary layer trailing edge noise spectra for the wall-mounted finite airfoil are normalized by both M^5 and suction side boundary layer displacement thickness δ_S^* in Fig. 5 (c) and (d):

$$Lp_{1/3\,\text{scaled2}} = Lp_{1/3} - 50\log_{10}(M) - 10\log_{10}(\delta_S^*), \tag{2}$$

and δ_S^* is used as the characteristic length scale. While boundary layer displacement thickness does not scale the level or frequency of peak contributions as well as the trailing edge thickness parameter, it does provide better scaling of the high frequency spectral region adjacent to the blunt vortex shedding and tip noise peaks. The noise levels at high frequencies ($St_{\delta_S^*} > 0.12$ for $\alpha = 0°$ and $St_{\delta_S^*} > 0.2$ for $\alpha = 6°$) collapse to within 6 dB when boundary layer displacement thickness is employed as the scaling parameter.

Figure 6 shows the 1/12th octave band spectra for the wall-mounted finite airfoil with natural boundary layer transition normalized by both M^5 and pressure side boundary layer displacement thickness δ_P^* according to

$$Lp_{1/3\,\text{scaled3}} = Lp_{1/3} - 50\log_{10}(M) - 10\log_{10}(\delta_P^*), \tag{3}$$

and δ_P^* is used as the characteristic length scale. Pressure side boundary layer displacement thickness is used as the normalisation parameter in this case as noise generation is linked with the presence of boundary layer instabilities in the transitional boundary layer that forms on the pressure side of the airfoil [4].

Despite the erratic nature of the tonal noise mechanism which leads to inconsistent spectral shape, Fig. 6 shows good collapse of the airfoil trailing edge noise spectra. At $\alpha = 0°$, spectral data that are originally spread by almost 35 dB are collapsed to within 10 dB (see Fig. 6 (a)). The level maxima of the noise spectra at flow speeds of $U_\infty = 40$ - 60 m/s all occur at a Strouhal number of $St_{\delta_P^*} = 0.12$.

At a higher angle of attack of $\alpha = 6°$, the spectra in Fig. 6 (b) coalesce to within 27 dB and display an increase in peak noise level with decreasing velocity. The peak noise level of the spectra at flow speeds of $U_\infty = 30$ - 50 m/s all occur at the same Strouhal number of $St_{\delta_P^*} = 0.052$.

4 Conclusions

This paper has examined the noise produced by a wall-mounted finite airfoil with tripped turbulent boundary layers and natural boundary layer transition. The results include sound maps taken with a microphone array and spectral data for the individual noise contribution from the

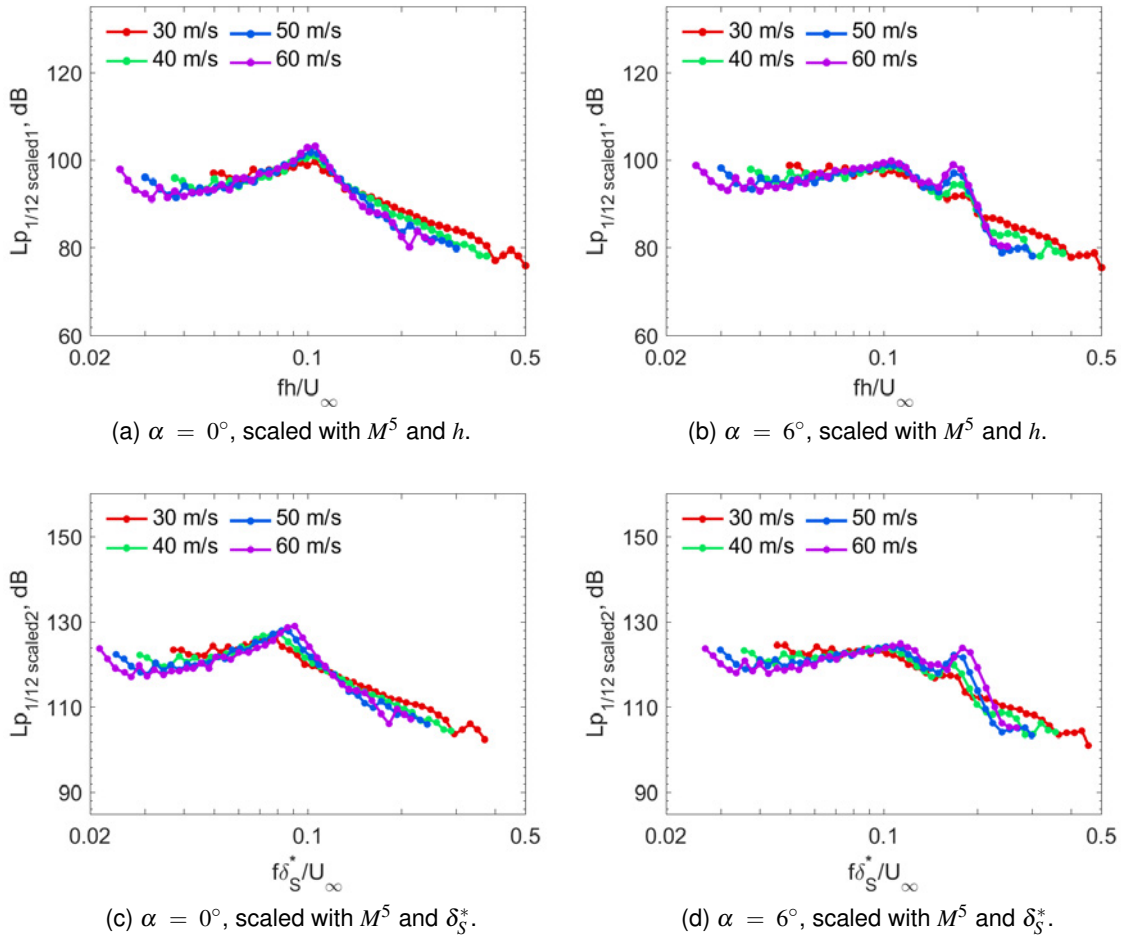

(a) $\alpha = 0°$, scaled with M^5 and h.

(b) $\alpha = 6°$, scaled with M^5 and h.

(c) $\alpha = 0°$, scaled with M^5 and δ_S^*.

(d) $\alpha = 6°$, scaled with M^5 and δ_S^*.

Figure 5: **Normalised 1/12th octave band trailing edge noise spectra for the tripped wall-mounted airfoil.**

airfoil trailing edge. Turbulent boundary layer trailing edge noise spectra are broadband in nature and feature a blunt vortex shedding noise component and a tip noise contribution. The trailing edge noise levels increase with M^5 in accordance with trailing edge theory and the frequency of the trailing edge noise scales with Strouhal number based on trailing edge thickness. With natural boundary layer transition, the trailing edge noise spectra contain a number of high amplitude peaks attributed to an aeroacoustic feedback loop between instabilities in the transitional boundary layer and acoustic waves produced at the trailing edge. The noise spectra scale well with an M^5 power law and pressure side boundary layer displacement thickness.

References

[1] Brooks, T.F.; Hodgson, T.H. Prediction and comparison of trailing edge noise using measured surface pressures. 6th AIAA Aeroacoustics Conference, Hartford, Conn., 4–6 June 1980.

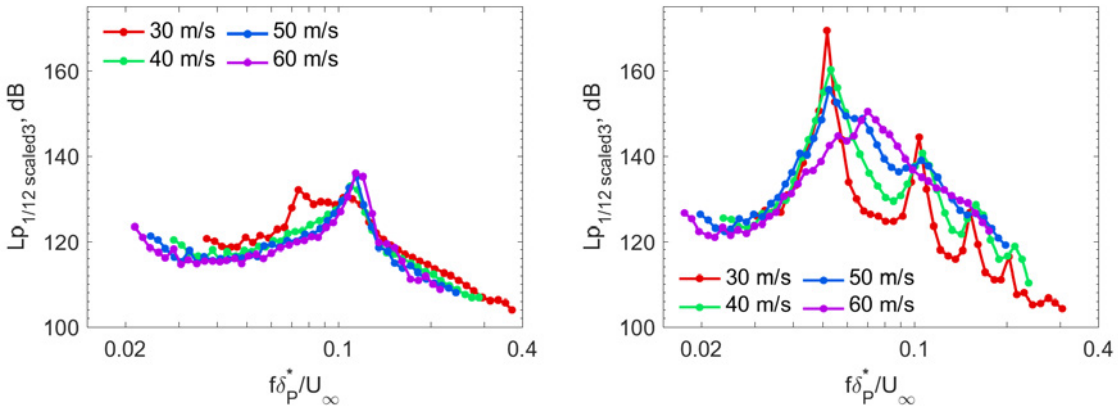

(a) $\alpha = 0°$, scaled with M^5 and δ_P^*.

(b) $\alpha = 6°$, scaled with M^5 and δ_P^*.

Figure 6: **Normalised 1/12th octave band trailing edge noise spectra for the untripped wall-mounted airfoil.**

[2] Arbey, H.; Bataille, J. Noise generated by airfoil profiles placed in a uniform laminar flow. Journal of Fluid Mechanics, 134, 1983, 33–47.

[3] Blake, W.K. Mechanics of Flow Induced Sound and Vibration, volume II: Complex flow-structure interactions, Academic Press, New York, 1986.

[4] Brooks, T.F.; Pope, D.S.; Marcolini, M. A. Airfoil self-noise and prediction. NASA Reference Publication 1218, 1989.

[5] Moreau, D.J.; Prime, Z.; Porteous, R.; Doolan, C.J.; Valeau, V. Flow-induced noise of a wall-mounted finite airfoil at low-to-moderate Reynolds number, Journal of Sound and Vibration, 333, 2014, 6924–6941.

[6] Moreau, D.J.; Doolan, C.J.; Alexander, W.N.; Meyers, T.W.; Devenport, W.J. Wall-mounted finite airfoil-noise production and prediction, AIAA Journal, 54(5), 2016, 1637–1651.

[7] Devenport, W.J.; Burdisso, R.A.; Borgoltz, A.; Ravetta, P.A.; Barone, M.F.; Brown, K.A.; Morton, M.A. The Kevlar-walled anechoic wind tunnel, Journal of Sound and Vibration, 332, 2013, 3971–3991.

[8] Drela, M. Xfoil: Subsonic airfoil development system, 2000, http://web.mit.edu/drela/Public/web/xfoil/. Site last visited 14/04/2016.

[9] Katz, J.; Plotkin, A. Low-speed Aerodynamics, 2nd Ed, Cambridge University Press, Cambridge UK, 2001.

[10] Ffowcs Williams, J.E.; Hall, L.H. Aerodynamic sound generation by turbulent flow in the vicinity of a scattering half plane, Journal of Fluid Mechanics, 40, 1970, 657–670.

[11] Herr, M.; Dobrzynski, W. Experimental investigations in low-noise trailing-edge design, AIAA Journal, 43(6), 2005, 1167–1175.